The Weakly Nonlinear Dynamics of a Planetary Green Mode and Atmospheric Vacillation*

BIN WANG

Geophysical Fluid Dynamics Program, Princeton University, Princeton, NJ 08542

ALBERT BARCILON

Geophysical Fluid Dynamics Institute and Department of Meteorology, Florida State University, Tallahassee, FL 32306

(Manuscript received 18 March 1985, in final form 3 February 1986)

ABSTRACT

Cold season atmospheric observations of vacillation point to a wave–mean flow interaction of baroclinic, planetary waves with their mean flow, and the observational data show that wave 2 is the largest contributor to the energetics and the heat flux. To verify this hypothesis we present a weakly nonlinear analysis of the evolution of a single, most unstable Green mode interacting with mean zonal flow in the presence of internal and Ekman layer dissipations, the former being larger than the latter.

The derived amplitude equations for the wave and the mean fields transform into a Lorenz set of equations that admits stable, finite amplitude wave states. No stable limit cycle or aperiodic solutions were found in the realistic parameter ranges that typify atmospheric winter conditions. When the system is disturbed away from these stable states, there is a monotonic or vacillatory approach to equilibrium. Damped vacillation occurs when the internal dissipative time scale is longer than the *e*-folding time scale of the inviscid, Green mode, a condition realized in the winter atmosphere. During the vacillation, due to the presence of the internal dissipation the tilt of the constant phase line may remain westward, and the horizontal heat flux may be poleward throughout most of the cycle.

1. Introduction

One of the features of the general circulation of the atmosphere on time scales of several weeks is the vacillation of the mean zonal energy and its associated eddy activities. Since Namias (1950) found zonal index oscillation with a periodicity ranging from 3 to 6 weeks, such fluctuations of various atmospheric variables have been investigated by many authors. These quasi-periodic variations are well documented in both the troposphere and the stratosphere and in both hemispheres; they appear to be related to the interaction between the westerlies and the planetary waves. During cold seasons, vacillations were found to be most likely linked to a baroclinic process (Miller, 1974; McGuirk and Reiter, 1976; McGuirk, 1982), while for non-winter seasons they seem to involve barotropic exchanges between zonal and eddy energies (Webster and Keller, 1975). By means of a numerical experiment, Yoden (1981) demonstrated that the baroclinic transfer may become prominent when the meridional heating increases. By using time series of simulated data generated from a hemispheric general circulation model, Hunt (1978) also obtained vacillatory behavior, particularly in the eddy kinetic and available potential energies, with a period of about 20 days. Apart from atmospheric observations and numerical simulations, the vacillations in wave amplitude and wave structure have also been well documented in laboratory annulus experiments (e.g., Pfeffer et al., 1974).

Theoretical or numerical studies of the physical processes or mechanisms capable of explaining various vacillatory behaviors of the atmospheric flow have been carried out by Arakawa (1961), Lorenz (1963a), Pedlosky (1970, 1979), Quinet (1974), and Yoden (1981), among others. Thus far, the majority of theoretical analysis dealing with wave–mean flow interaction has considered Ekman dissipation with less attention given to internal thermal dissipation. Pedlosky (1979) studied the weakly nonlinear dynamics of the Charney mode in the presence of Ekman dissipation and Newtonian cooling. If we denote by δ, μ measures of the Ekman dissipation and internal dissipation due primarily to Newtonian cooling, respectively, and if Δ is a measure of the supercriticality ($\Delta \ll 1$), the cases investigated by Pedlosky correspond to $\delta = O(\Delta^{1/2})$, $\mu \ll \Delta$ and $\delta = O(1)$, $\mu = O(\Delta)$. Physically, the latter regime dealt with an Ekman spindown time scale which is much shorter, and an internal dissipation time scale that is much longer than the baroclinic development time

* Contribution No. 230 of Geophysical Fluid Dynamics Institute, Florida State University.

scale. For ultralong planetary waves under atmospheric winter conditions a regime in which the internal dissipation plays a dominant role is more likely to prevail. Since the planetary waves have their large wave amplitude in the upper troposphere and stratosphere and rather small amplitude near surface, the Ekman dissipation, that is proportional to the vorticity at the top of Ekman layer, is not an efficient energy sink for these waves. Besides, the available potential energy of the planetary wave is much larger than its kinetic energy and the contribution to the eddy potential vorticity due to the thermal field is much larger than that due to the relative vorticity. Therefore, the internal thermal dissipation becomes an efficient energy sink in the dynamics of these planetary waves. By using a three-layer model based upon the Burger equations, one of the authors (Wang, 1982) found that, when the internal dissipation exceeds $1/\sqrt{2}$ times the e-folding, inviscid baroclinic time scale, the nonlinear thermal advection produced damped oscillations of the zonal potential energy. Yet, his model lacked vorticity advection and was unable to cope with the intricate vertical structure of these modes.

The present study pertains to the weakly nonlinear evolution of the diabatic, transient planetary waves, their interaction with the zonal mean flow, and the role played by this interaction in atmospheric vacillation. For typical winter conditions, the slowly eastward propagating planetary waves (wave two, three, and four) may be viewed as the atmospheric counterpart of the strongly unstable Green mode (Wang et al., 1985; hereafter WBH). We propose to extend the linear Charney model into the weakly nonlinear regime and examine the dynamics of a single most unstable Green mode in an effort to verify some of the observational findings pertaining to the vacillation of the westerlies in cold season.

Section 2 deals with the model formulation; the reader not interested in the asymptotic techniques used in solving this problem may omit section 3, which briefly summarizes the results derived by these techniques. Section 4 describes the amplitude equations, their equilibrium states, the linear stability of these equilibria, and the behavior of the solution as these steady states are approached. Finally, possible applications to atmospheric vacillation are discussed in section 5.

2. The model

We examine the stability of a basic zonal flow with a constant vertical shear λ_* and no meridional variation. We assume a basic state density distribution, $\rho_s = \rho_s(0)\exp(-z_*/H)$ and a constant Brunt–Väisälä frequency N, where H denotes the density scale height, approximated by a constant. The zonal flow, which extends to infinity in the vertical, is confined to a midlatitude β-plane channel of width $2L$. The implications and limitations of the β-plane channel approximation have been discussed by Pedlosky (1979) and WBH. A planetary scale, wavelike perturbation having a single zonal wavenumber is presumed to be imposed on the basic flow. Since the evolution of the planetary waves is characterized by a longer time scale, diabatic heating and mechanical dissipations should be included in the model. We shall assume that the Newtonian cooling and horizontal turbulent diffusion of the momentum act as internal dissipations on the potential vorticity in the interior region (above the frictional Ekman layer) and express these by means of a Rayleigh term in the potential vorticity equation. The Ekman layer dissipation is included via the lower boundary condition for the interior motion. The limitations of these assumptions will be discussed further on.

If we scale x_*, y_* by L, z_* by H, the horizontal velocity by $V = \lambda_* H$, t_* by advective time scale L/V, and the streamfunction ϕ_* by LV, the nondimensional potential vorticity equation for the perturbation field ϕ, after multiplication by the Burger number S, takes the form

$$\left(\frac{\partial}{\partial t} + z\frac{\partial}{\partial x}\right)q + b\frac{\partial \phi}{\partial x} + J(\phi, q) = -\mu q, \quad (2.1)$$

where

$$q = \left(\frac{\partial^2}{\partial z^2} - \frac{\partial}{\partial z} + S\nabla^2\right)\phi \quad (2.2)$$

represents the perturbation potential vorticity times the Burger number

$$S = \frac{N^2H^2}{f_0^2L^2}; \quad (2.3a)$$

b is the basic-state potential vorticity gradient multiplied by the Burger number, which will be referred to as modified potential vorticity gradient, and is given by

$$b = 1 + \frac{1}{\lambda}. \quad (2.3b)$$

We took the density scale height as the vertical scale; so that, in (2.3b), the first term of rhs denotes the mass convergence effect,

$$\lambda = \frac{\lambda_* f_0^2}{\beta_* N^2 H} \quad (2.3c)$$

is a nondimensional vertical shear that measures the competitive effects of the baroclinic vortex stretching vs the β-effect in producing potential vorticity; μ is a nondimensional internal dissipation coefficient

$$\mu = \frac{L}{V\tau_*},$$

where τ_* is a typical internal dissipation time. For the planetary scale motion the thermal field makes the major contribution to the potential vorticity and the Newtonian cooling is the dominant contribution to

the internal dissipation of the potential vorticity field. We shall regard τ_* as Newtonian cooling time in what follows.

The vertical velocity at the lower boundary is assumed to match the Ekman pumping velocity, and the lower boundary condition is

$$\frac{\partial^2\phi}{\partial t\partial z} - \frac{\partial\phi}{\partial x} + J\left(\phi, \frac{\partial\phi}{\partial z}\right) + \mu\frac{\partial\phi}{\partial z} + \delta\nabla^2\phi = 0, \quad \text{at} \quad z = 0, \quad (2.4a)$$

where δ, a measure of the Ekman dissipation, is defined by

$$\delta = \frac{N^2H}{f_0LV}\left(\frac{A_v}{2f_0}\right)^{1/2};$$

A_v is the vertical turbulent viscosity coefficient. As $z \to \infty$, the upward energy flux vanishes. This implies

$$\lim_{z\to\infty}\int_{-1}^{1}\rho_s \times \overline{\phi\left[\left(\frac{\partial}{\partial t} + z\frac{\partial}{\partial x}\right)\frac{\partial\phi}{\partial z} - \frac{\partial\phi}{\partial x} + J\left(\phi, \frac{\partial\phi}{\partial z}\right) + \mu\frac{\partial\phi}{\partial z}\right]} \times dy = 0. \quad (2.4b)$$

At the side walls of the channel the meridional velocity must vanish, and, for consistency, we must also require that

$$\overline{\frac{\partial^2\phi}{\partial t\partial y}} = \lim_{X\to\infty}\frac{1}{2X}\int_{-X}^{X}\frac{\partial^2\phi}{\partial t\partial y}dx = 0, \text{ at } y = \pm 1. \quad (2.4c)$$

The linear problem was analyzed in detail by WBH. Neutral modes are found when

$$b = b_c = 2n\tilde{K}, \quad n = 1, 2, 3, \cdots$$

where $\tilde{K}$ is the total horizontal wavenumber modified by the mass convergence effect, and is defined by

$$\tilde{K}^2 = SK^2 + \tfrac{1}{4}. \quad (2.5)$$

The Charney modes are found for $0 < b < 2\tilde{K}$; the Green modes lie in $2\tilde{K} < b < 4\tilde{K}$, while the Burger modes are associated with $b > 4\tilde{K}$ but $b/\tilde{K}$ different from any even integer. To the right of $b = b_c$ weak instabilities exist while to the left of $b = b_c$ strong instabilities prevail. To focus our attention on the planetary scale disturbances during winter conditions, we consider their model counterparts, the strongly unstable Green modes. More precisely, we rewrite b in the vicinity of $b_c = 4\tilde{K}$ as

$$b = 2\tilde{K}(2 - \Delta), \quad (2.6)$$

where

$$\Delta = \frac{(4\tilde{K} - 1)}{2\tilde{K}}\frac{(\lambda - \lambda_c)}{\lambda} > 0, \quad \lambda_c = \frac{1}{4\tilde{K} - 1}. \quad (2.7)$$

Since $(4\tilde{K} - 1)/2\tilde{K}$ is an O(1) quantity, Δ is a measure of the shear supercriticality. WBH showed that the most unstable, linear Green mode is found when $\Delta \approx 0.3$.

We introduce a parameter ϵ that measures the wave amplitude and let $\Delta = O(\epsilon)$. The asymptotic expansions will be expressed in terms of ϵ which is assumed to be small. The relative importance of the internal dissipation versus Ekman dissipation is given by the ratio of μ to δ:

$$\frac{\mu}{\delta} = \frac{L^2}{L_D{}^2}\cdot\frac{H}{\tau_*}\left(\frac{2}{f_0A_v}\right)^{1/2}, \quad (2.8)$$

where $L_D = NH/f_0$ is the Rossby radius of deformation. Equation (2.8) indicates that the internal dissipation may become a major energy sink when the horizontal length scale increases. This is especially true for the Green mode which has a large temperature perturbation in the upper troposphere or lower stratosphere with small vorticity fluctuations near the ground. Therefore, we set

$$\mu = O(\Delta^{1/2}), \quad \delta = O(\Delta) \quad (2.9)$$

in view of its dynamical relevance to planetary scale Green waves during cold seasons. Equation (2.9) implies that the internal dissipative time scale is of the same order of magnitude as the e-folding time of inviscid baroclinic growth, and that the Ekman spindown time scale is much longer than the baroclinic development time scale.

3. Amplitude equations

As shown by Pedlosky (1970), a regular perturbation expansion is not uniformly valid in time, and a slow time $T = \Delta^{1/2}t$ must be introduced. Because $\Delta \ll 1$ we are close to the critical point and the fast time will not enter the problem. Then, near the Green critical point, (2.1) becomes

$$\left(\Delta^{1/2}\frac{\partial}{\partial T} + z\frac{\partial}{\partial x} + \mu\right)q + (4\tilde{K} - 2\tilde{K}\Delta)\frac{\partial\phi}{\partial x} + J(\phi, q) = 0. \quad (3.1)$$

The problem is not uniformly valid in z either, as can be seen by considering the linear advective operator $(\Delta^{1/2}\partial/\partial T + z\partial/\partial x + \mu)$ which becomes much smaller than O(1) as $z \to 0$. Therefore, a boundary layer of thickness $O(\epsilon^{1/2})$ is needed near $z = 0$. Thus, the problem must be solved in terms of an interior solution, which satisfies the lateral boundary conditions as well as the condition at $z = \infty$, and a boundary layer solution, which satisfies the lateral conditions as well as the boundary condition at $z = 0$. The two solutions must then be matched (Pedlosky, 1979).

Let

$$\phi = \sum_{n=1}^{\infty}\epsilon^{n/2}\phi_{n-1}(x, y, z, T), \quad (3.2a)$$

$$q = \sum_{n=1}^{\infty} \epsilon^{n/2} q_{n-1}(x, y, z, T) \tag{3.2b}$$

be the interior solution. We substitute (3.2) into (3.1), gather like powers of ϵ, and obtain a sequence of linear equations at various orders; the lowest order equation admits a solution of the form

$$\phi_0 = \tilde{\phi}_0 = A(T)\varphi_0(z)W + \text{c.c.} \tag{3.3}$$

where the tilde denotes a wave field and c.c. denotes "complex conjugate". We have introduced

$$W = e^{ikx}\cos ly, \quad l = \left(m + \frac{1}{2}\right)\pi, \quad m = 0, 1, 2, \cdots,$$

$$\varphi_0(z) = z(1 - \tilde{K}z)e^{pz}, \quad p = \frac{1}{2} - \tilde{K} < 0, \tag{3.3a}$$

where $\varphi_0(z)$ is the z-structure of the neutral Green mode; $A(T)$ is the yet unknown complex amplitude of the weakly nonlinear Green mode. The solution for ϕ_1, which is bounded at infinity, is

$$\phi_1 = \bar{\phi}_1(y, z, T) + \frac{1}{ik}\mathcal{L}A(1 - 2\tilde{K}z)e^{pz}W + \text{c.c.}, \tag{3.4}$$

where,

$$\mathcal{L} \equiv \frac{\Delta^{1/2}}{\epsilon^{1/2}}\frac{\partial}{\partial T} + \frac{\mu}{\epsilon^{1/2}} \tag{3.4a}$$

and the mean flow correction, $\bar{\phi}_1(y, z, T)$, remains to be determined.

Within the boundary layer near $z = 0$, we introduce a stretched coordinate $\zeta = z/\epsilon^{1/2}$ and let $\hat{\phi}(x, y, \zeta, T)$ be the boundary layer streamfunction. Equation (3.1) and lower boundary condition (2.4a) can then be expressed in terms ζ and $\hat{\phi}$. Let

$$\hat{\phi} = \epsilon\hat{\phi}_1(x, y, \zeta, T) + \epsilon^{3/2}\hat{\phi}_2(x, y, \zeta, T) + \cdots.$$

We insert this expansion into the boundary layer equation and boundary condition at $z = 0$, collect like powers of $\epsilon^{1/2}$, and obtain the $\hat{\phi}_1$- and $\hat{\phi}_2$-problems, from which one finds that the boundary layer solution to $O(\epsilon^2)$ is

$$\begin{aligned}\hat{\phi}(x, y, \zeta, T) &= \epsilon\left[\left(\zeta + \frac{1}{ik}\mathcal{L}\right)D_1(T)W + \text{c.c.} + \tilde{\bar{\phi}}_1(y, T)\right] + \epsilon^{3/2} \\ &\times \left\{\left[\frac{D_1}{2}(1 - 4\tilde{K})\zeta^2 + D_2(T)\zeta + \frac{1}{ik}\mathcal{L}D_2 - D_1\frac{\partial\tilde{\bar{\phi}}_1}{\partial y}\right]\right. \\ &\left. \times W + \text{c.c.} + \zeta\bar{E}_1(y, T) + \bar{E}_2(y, T)\right\} + O(\epsilon^2). \end{aligned} \tag{3.5}$$

where $\tilde{\bar{\phi}}_1$, $\bar{E}_1$, $\bar{E}_2$ as well as D_1, D_2 are functions that do not depend on x and are determined by the matching conditions. Writing (3.2a) along with (3.3) and (3.4) in terms of ζ and expanding in powers of $\epsilon^{1/2}$ and matching with (3.5), we find

$$\begin{aligned} D_1(T) &= A(T), \\ D_2(T) &= ik(2\tilde{K} - p)\mathcal{L}A(T), \\ \tilde{\bar{\phi}}_1(y, T) &= \bar{\phi}_1(y, 0, T), \\ \bar{E}_1(y, 1) &= \frac{\partial\bar{\phi}_1}{\partial z}(y, 0, T), \end{aligned}$$

$$\phi_2(x, y, 0, T) = \left[\frac{2\tilde{K} - p}{k^2}\mathcal{L}^2A - A\frac{\partial\bar{\phi}_1}{\partial y}(y, 0, T)\right] \times W + \text{c.c.} + \bar{E}_2(y, T). \tag{3.6}$$

To determine the dependence of the wave amplitude and mean flow correction on the slow time scale T, we now investigate the higher order ϕ_2-problem, given by

$$\frac{\partial}{\partial x}(zq_2 + 4\tilde{K}\phi_2) = -\mathcal{L}q_1 + 2\frac{\Delta}{\epsilon}\tilde{K}\frac{\partial\phi_0}{\partial x} - J(\phi_0, q_1) - J(\phi_1, q_0). \tag{3.7}$$

We write

$$\phi_2 = \bar{\phi}_2(y, z, T) + \tilde{\phi}_2(x, y, z, T),$$

$$q_j = \tilde{q}_j(x, y, z, T) + \bar{q}_j(y, z, T), \quad j = 1, 2,$$

and perform an x-average of (3.7) to find the governing equation for the mean flow correction, $\bar{u}_1 = -\partial\bar{\phi}_1/\partial y$,

$$\mathcal{L}\left(\frac{\partial^2}{\partial z^2} - \frac{\partial}{\partial z} + S\frac{\partial^2}{\partial y^2}\right)\bar{u}_1 = 8\tilde{K}l^2\mathcal{L}|A|^2\frac{\varphi_0^2}{z^2}\cos 2ly, \tag{3.8}$$

where $\bar{u}_1 \to 0$, as $z \to \infty$ and, from (2.4c),

$$\frac{\partial\bar{u}_1}{\partial T} = 0, \quad \text{at} \quad y = \pm 1. \tag{3.9}$$

Using (3.5) and the matching result in the boundary condition of $\hat{\phi}_2$-problem, and after performing an x-average, we get,

$$\mathcal{L}\frac{\partial\bar{u}_1}{\partial z} = -2l^2\left(\mathcal{L} + \frac{\mu}{\epsilon^{1/2}}\right)|A|^2\cos 2ly, \quad \text{at} \quad z = 0, \tag{3.10}$$

which constitutes the boundary condition at $z = 0$ for the $\bar{u}_1$ field. We also take $\bar{u}_1 = 0$ at $T = 0$. From (3.8) and (3.10), the time and spatial dependences separate, and we can assume a solution of the form

$$\bar{u}_1(y, z, T) = \sum_{J=1}^{\infty} B(T)f_J(z)\cos jy, \tag{3.11}$$

where $j = (J - \frac{1}{2})\pi$, $J = 1, 2, \cdots$ so that the lateral boundary conditions are automatically satisfied. After we substitute (3.11) into (3.8), separate the time and spatial dependences, we obtain the time evolution equation for $B(T)$,

$$\left(\frac{d}{dT}+\frac{\mu}{\Delta^{1/2}}\right)B=\left(\frac{d}{dT}+2\frac{\mu}{\Delta^{1/2}}\right)|A|^2. \quad (3.12)$$

The Appendix gives the solution for the vertical structure functions $f_J(z)$.

Removing the mean flow component from (3.7) leads to an interior differential equation for the wave component $\tilde{\phi}_2(x, y, z, T)$. To eliminate nonuniformities in the asymptotic expansion, we impose the solvability condition to $\tilde{\phi}_2$-equation, i.e., we multiply the $\tilde{\phi}_2$-equation by $\varphi_0(z)e^{-z}W^*/z$, where W^* is the complex conjugate of W, and integrate over the entire domain of the model. Making use of the expression for $\varphi_0(z)$, (3.3a), the lower boundary condition (3.6), and further substituting the mean flow correction (3.11) into the solvability condition, we finally obtain the governing equation for the wave amplitude evolution:

$$\frac{d^2A}{dT^2}+2\frac{\mu}{\Delta^{1/2}}\frac{dA}{dT}-\frac{k^2C_{0I}^2-\mu^2}{\Delta}A+\chi AB=0, \quad (3.13)$$

where

$$C_{0I}=\Delta^{1/2}/[4\tilde{K}(\tilde{K}-p)]^{1/2}$$

represents the imaginary part of the phase speed for the linear, inviscid Green mode, the quantity χ is given by (A3) in the Appendix.

4. The behavior of the dynamic system

a. General remarks

The dependence of the wave amplitude and mean flow correction on the slow time is governed by (3.12) and (3.13) with $B(0) = 0$, $A(0)$ given. In (3.13), the quantity χ measures the nonlinear feedback between the wave and the mean flow correction. Although the expression for χ, as given in the Appendix, is complicated, it nevertheless depends only on k, l once we fix S, ϵ and Δ. Numerical calculations show that a few terms of the series provide a very accurate representation for χ. For example, when the lowest and next to the lowest y-modes are retained, errors of 1% are found when two and six terms, respectively, are retained. Figure 1 shows the dependence of χ on the wavenumbers k, l. It is seen that χ is positive for all the (Green) modes and it increases as k, l increase. The positiveness of χ implies that the nonlinear feedback in (3.13) is *stabilizing*, a feature we shall discuss in more detail later.

In general, the amplitude A can be complex. Letting $A(T) = R(T)e^{-i\theta(T)}$, we can rewrite (3.12) and (3.13) as

$$\frac{d^2R}{dT^2}+\frac{2\mu}{\Delta^{1/2}}\frac{dR}{dT}-\frac{k^2C_{0I}^2-\mu^2}{\Delta}R+\chi RB-R\left(\frac{d\theta}{dT}\right)^2=0,$$

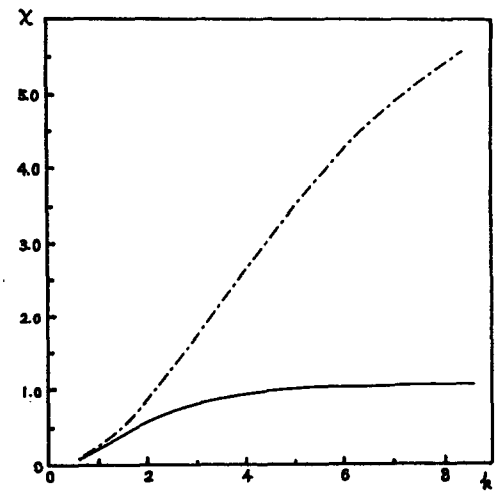

FIG. 1. Coefficient χ as a function of wavenumber k for the Green modes. The solid (dot–dashed) line is calculated for $l = \pi/2$ ($l = 3\pi/2$).

$$\frac{d^2\theta}{dT^2}+2\frac{d\theta}{dT}\frac{d\ln R}{dT}+\frac{2\mu}{\Delta^{1/2}}\frac{d\theta}{dT}=0,$$

$$\frac{dB}{dT}+\frac{\mu}{\Delta^{1/2}}B-2R\frac{dR}{dT}-2\frac{\mu}{\Delta^{1/2}}R^2=0. \quad (4.1)$$

The first integral of the second equation in (4.1) is

$$\frac{d\theta}{dT}=\frac{d\theta(0)}{dT}\frac{R^2(0)}{R^2}e^{-(2\mu/\Delta^{1/2})T}. \quad (4.2)$$

Assume that the mean flow has no correction initially, i.e., $B(0) = 0$, and the initial amplitude is real, $R(0) = R_0$, $\theta(0) = 0$, i.e., $A(0) = R_0$. The initial condition for dR/dT and $d\theta/dT$ will be assumed to be given by linear theory, i.e.,

$$\frac{dR(0)}{dT}=\frac{kC_I}{\Delta^{1/2}}R_0,$$

$$\frac{d\theta(0)}{dT}=\frac{kC_R}{\Delta^{1/2}}, \quad (4.3)$$

where C_I and C_R are the imaginary and the real parts of the complex phase speed as predicted by linear theory. According to WBH [their (4.6)], in the presence of internal dissipation, for strongly unstable Green modes ($\Delta > 0$, $n = 2$), we have

$$C_R=\frac{\Delta}{8\tilde{K}}\frac{(8\tilde{K}-1)}{(4\tilde{K}-1)}+O(\Delta^{3/2})=O(\Delta),$$

$$C_I=-\frac{\mu}{k}+C_{0I}+O(\Delta^{3/2}\ln\Delta^{1/2})=O(\Delta^{1/2}). \quad (4.4)$$

It follows that $d\theta(0)/dT$ is an $O(\Delta^{1/2})$ quantity, where $dR(0)/dT$ is $O(1)$. Since $d\theta/dT$ decays exponentially [see (4.2)], the last term in the left-hand side of the first equation in (4.1) is $O(\Delta)$ which is much smaller than

the other terms that are O(1). If we neglect this higher order quantity initially by assuming $d\theta(0)/dT = 0$, then $\theta = 0$, and the complex amplitude A remains real. Numerical integration of (4.1) indicates that the influence of the variation of wave phase, θ, on $R(T)$ is negligible, though $\theta(T)$ does exhibit an out-of-phase vacillation when compared to $R(T)$.

Based upon the preceding discussion we assume that A is real. The transformation

$$\tau = \frac{\mu}{\Delta^{1/2}} T, \quad X = \Delta^{1/2} A \frac{\sqrt{2\chi}}{\mu},$$
$$Z = \frac{\chi\Delta}{\mu^2} B, \quad Y = X + \frac{dX}{d\tau} \tag{4.5}$$

takes (3.12), (3.13) into the following form

$$\left.\begin{aligned} \frac{dX}{d\tau} &= -X + Y \\ \frac{dy}{d\tau} &= -XZ + rX - Y \\ \frac{dz}{d\tau} &= XY - Z \end{aligned}\right\}, \tag{4.6}$$

where the only nondimensional parameter entering the problem is

$$r = \frac{k^2 C_{0I}^2}{\mu^2}, \tag{4.6a}$$

which measures the ratio of the inviscid growth rate versus the internal damping rate. Equations (4.6) are a special case of the Lorenz set of equations (1963b) for unit Prandtl number, unit aspect ratio, and the Rayleigh number equals r. Lorenz showed that for large Rayleigh numbers (i.e., $r = 28$), the solutions are unsteady, aperiodic and highly sensitive to the initial conditions. They are therefore unpredictable.

Since application of the Lorenz set of equations to the real atmosphere required the use of severe truncation in the spectral representation of the model, efforts were made by, e.g., Brindley and Moroz (1980), Pedlosky (1980) to show that the amplitude evolution equation for weakly nonlinear baroclinic waves in the presence of small Ekman layer dissipation might possess similar behaviors as those of the Lorenz set. As Brindley and Moroz pointed out, in order to fit the side-wall boundary conditions, a Fourier expansion for the mean flow correction is needed, and hence the equations are transformed into an infinite set, which is obviously not the Lorenz set. In the two-layer or Eady model the waves are nondispersive due to the absence of the basic state potential vorticity gradient, say the β-effect. Again, if the β-effect were included in the model, the resultant amplitude equations, for β small, become a set of ordinary differential equations with complex coefficients, and these equations seem to behave differently from the Lorenz equations. Here, the amplitude equations, derived from a continuously stratified model with a planetary vorticity gradient, and with the presence of internal dissipation, can be cast into the Lorenz system in which r is the only parameter. However, because of the parameter setting, the behavior of these amplitude equations is quite different from that of the Lorenz set, as will be shown below.

b. *Equilibrium states and their stability*

Equations (4.6) possess the trivial solution $X = Y = Z = 0$ which corresponds to the wave-free basic state with a linear shear. A linear perturbation around that equilibrium state yields a characteristic equation

$$(\Gamma + 1)(\Gamma^2 + 2\Gamma + 1 - r) = 0,$$

which has three real roots if $r > 1$, with one positive root ($\Gamma = -1 + \sqrt{r}$). This equilibrium is then unstable. The condition $r > 1$ implies that

$$C_I = -\frac{\mu}{k} + C_{0I} = -\frac{\mu}{k} + \left(\frac{\Delta}{4\tilde{K}(\tilde{K} - p)}\right)^{1/2} > 0,$$

i.e., in the presence of internal dissipation there exists a growing, baroclinic Green mode. These results confirm those of linear theory.

For $r > 1$, there are two additional equilibrium solutions given by $X_e = Y_e = \pm\sqrt{r - 1}$, and $Z_e = r - 1$, implying that

$$A_e = \pm[(k^2 C_{0I}^2 - \mu^2)/2\chi\Delta]^{1/2},$$
$$B_e = (k^2 C_{0I}^2 - \mu^2)/\chi\Delta. \tag{4.7}$$

A linear stability analysis in the vicinity of these equilibrium points yields a characteristic equation of the form

$$\Gamma^3 + 3\Gamma^2 + (r + 1)\Gamma + 2(r - 1) = 0.$$

This equation has one real, negative root and two complex conjugate roots. It can be shown that all $\mathrm{Re}\Gamma < 0$ so that *both* of these equilibrium points are always stable to small perturbations. With the use of (4.7) we can write the equilibrated streamfunction as

$$\psi_e = -yz - \epsilon \frac{k^2 C_{0I}^2 - \mu^2}{\chi\Delta} \sum_{j=1}^{\infty} j \sin jy \cdot f_j(z) + \epsilon^{1/2}$$
$$\times \left(\frac{k^2 C_{0I}^2 - \mu^2}{2\chi\Delta}\right)^{1/2} \left[z(1 - \tilde{K}z) - \frac{i}{k}\mu(1 - 2\tilde{K}z)\right]$$
$$\times e^{2pz} \cos kx \cos ly + O(\epsilon^{3/2}). \tag{4.8}$$

This contains a standing wave term, proportional to $[(k^2 C_{0I}^2 - \mu^2)/2\chi\Delta]^{1/2}$ and a rectified mean field term, proportional to $\epsilon(k^2 C_{0I}^2 - \mu^2)/\chi\Delta$. The amplitudes of both terms depend on the quantity Δ, a measure of the shear supercriticality, and on $(k^2 C_{0I}^2 - \mu^2)$, a measure of the competitive effect of the inviscid baroclinic growth rate vs the internal damping. These amplitudes

are also inversely proportional to powers of χ, a quantity that decreases as k and l decrease. Thus, the steady, standing wavelike equilibrium states will reach their largest amplitude when χ is small, i.e., for planetary waves with small k, say wave 2, and with the lowest y-mode. We then speculate that the planetary waves play a more important role than the cyclone waves in the long term variations of the westerlies. Another feature of interest is that the equilibrium state given by (4.8) is independent of the initial conditions.

Figure 2 depicts the vertical structure of the mean flow correction at the equilibrium state for different latitudes (i.e., different values of y). The largest changes occur near the central latitude of the channel. At that latitude the mean velocity increases near the ground and decreases in the stratosphere so that the vertical shear of the initial basic state is reduced.

c. *Evolution toward the equilibrium states*

With the relaxation of the side wall boundary conditions, for the two layer, f-plane model, Pedlosky (1971) derived evolution equations of the form

$$\frac{d^2R}{d\theta^2} + \alpha\eta\frac{dR}{d\theta} - R + R(R^2 - D) = 0,$$

$$\frac{dD}{d\theta} + \eta D + \beta\eta R^2 = 0 \tag{4.9}$$

where R is the wave amplitude, D is related to the mean flow correction amplitude, η is a measure of the Ekman dissipation, and α, β are functions of the wavenumbers only. In a later paper, Pedlosky (1972) was able to show that, for small η, the limit cycle solutions (either stable or unstable) are possible only for a restricted range of α/β, the upper limit of which, deduced by first-order approximate expansion, was found to be

$$\alpha/\beta = 2\text{–}3E(1)/K(1) = 2.0,$$

where $K(\kappa)$ and $E(\kappa)$ are the complete elliptic integrals of the first and second kind, respectively.

If we let

$$R = A\left(\frac{\chi\Delta}{k^2C_{0I}^2 - \mu^2}\right)^{1/2}, \quad D = (A^2 - B)\frac{\chi\Delta}{k^2C_{0I}^2 - \mu^2},$$

$$\theta = T\left(\frac{k^2C_{0I}^2 - \mu^2}{\Delta}\right)^{1/2}, \tag{4.10}$$

we verify that substitution of (4.10) into (4.9) yields our dynamic system, (3.12) and (3.13), provided

$$\alpha = 2, \quad \beta = 1,$$

$$\eta = \mu/(k^2C_{0I}^2 - \mu^2)^{1/2}. \tag{4.11}$$

In terms of Pedlosky's criteria for an approximate solution, it is difficult to infer the type of dynamical behavior for our system since $\alpha/\beta = 2$. Numerical integration seems to indicate that there is no stable limit cycle for values of μ ranging between 10^{-1} and 10^{-4} and for values of the initial wave amplitude, A_0, ranging from 0.1 to 1.5.

Although perpetual vacillation was not found numerically in our model, a vacillatory behavior *may* emerge as the system approaches its steady state. To understand the nature of the evolution towards the equilibrium state, let us reconsider the *local behavior* of the system (3.12) and (3.13) in the vicinity of the equilibrium state, where $B = 2A^2$. Writing $y_1 = dA/dT$, $y_2 = A$, (3.13) with A real, becomes

$$\frac{dy_1}{dT} = -\frac{2\mu}{\Delta^{1/2}}y_1 + \frac{k^2C_{0I}^2 - \mu^2}{\Delta}y_2 - 2\chi y_2^3,$$

$$\frac{dy_2}{dT} = y_1. \tag{4.12}$$

These equations have the nontrivial steady solution $y_1^{(s)} = 0$, $y_2^{(s)} = \pm[(k^2C_{0I}^2 - \mu^2)/2\chi\Delta]^{1/2}$. Since $y_2 = A$, only the positive root is physically meaningful. In the vicinity of the equilibrium state corresponding to that root the system (4.12) may be written as

$$\frac{d\tilde{X}}{dT} = \tilde{A}X + \tilde{R}(X), \tag{4.13}$$

where

$$\tilde{X} = \begin{pmatrix} x_1 \\ x_2 \end{pmatrix} = \begin{pmatrix} y_1 \\ y_2 - y_2^{(s)} \end{pmatrix},$$

$$\tilde{A} = \begin{pmatrix} -\dfrac{2\mu}{\Delta^{1/2}} & -2\dfrac{k^2C_{0I}^2 - \mu^2}{\Delta} \\ 1 & 0 \end{pmatrix}$$

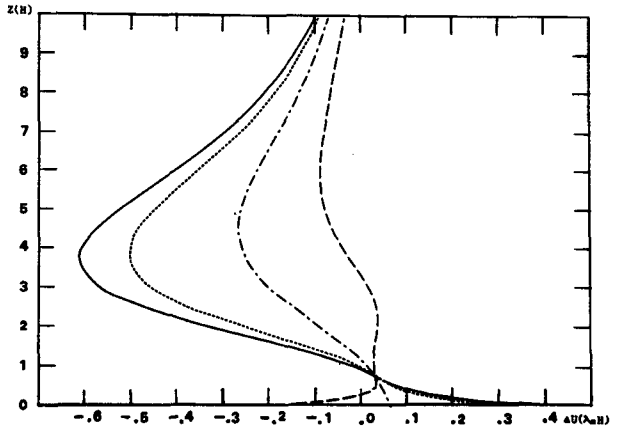

FIG. 2. The mean flow correction for the equilibrium wave state, ΔU, as a function of height, z, for wave two. Parameters used in the calculation are $\theta_0 = 45°$, $L_y = 5500$ km, $N = 0.017$ s^{-1}, $\lambda_* = 0.0013$ s^{-1}, $l = \pi/2$, $\mu = 0.05$, and $\Delta = 0.28$. The solid, dotted, dot–dashed, and dashed lines are calculated at $y = 0$, ±0.25, ±0.50, ±0.75, respectively.

is the coefficient matrix of the so-called first approximation equation, which is nonsingular; $\tilde{R}(X)$ denotes the nonlinear term. For this steady solution $(y_1^{(s)}, y_2^{(s)})$, the properties of the solution nearby depend upon the eigenvalue of $\tilde{A}$ only. The characteristic equation of $\tilde{A}$ is

$$\lambda^2 + 2\frac{\mu}{\Delta^{1/2}}\lambda + 2\frac{(k^2C_{0I}^2 - \mu^2)}{\Delta} = 0.$$

When $\mu \geq \sqrt{2/3}kC_{0I}$, this characteristic equation possesses two nonzero real roots indicating that the approach to equilibrium is *monotonic*. When

$$\mu < \sqrt{2/3}\, kC_{0I} \tag{4.14}$$

there are two complex conjugate roots having a negative real part. The singularity is a stable focus. In a phase plane portrait, the solution trajectories spiral about the steady solution i.e., the approach is *oscillatory*. The preceding criterion controls the monotonic or the oscillatory approach to the steady state and involves the competition between the inviscid growth rate kC_{0I} for baroclinic, unstable Green modes, and the internal dissipation due to Newtonian cooling and horizontal diffusion of momentum. For a typical winter atmosphere, the baroclinic development time for the Green mode is roughly three times that of the Charney mode (WBH, 1985); i.e., it is less than one week while the Newtonian cooling time is about 3–4 weeks, implying that, in practice, (4.14) is satisfied and the approach to equilibrium is oscillatory.

To verify the above qualitative conclusions, we integrated (3.12) and (3.13) numerically by using a fourth-order Runge-Kutta method with time step $\Delta T = 0.02$. Figures 3a, b show a representative damped oscillatory evolution of the wave amplitude when the criterion (4.14) is satisfied.

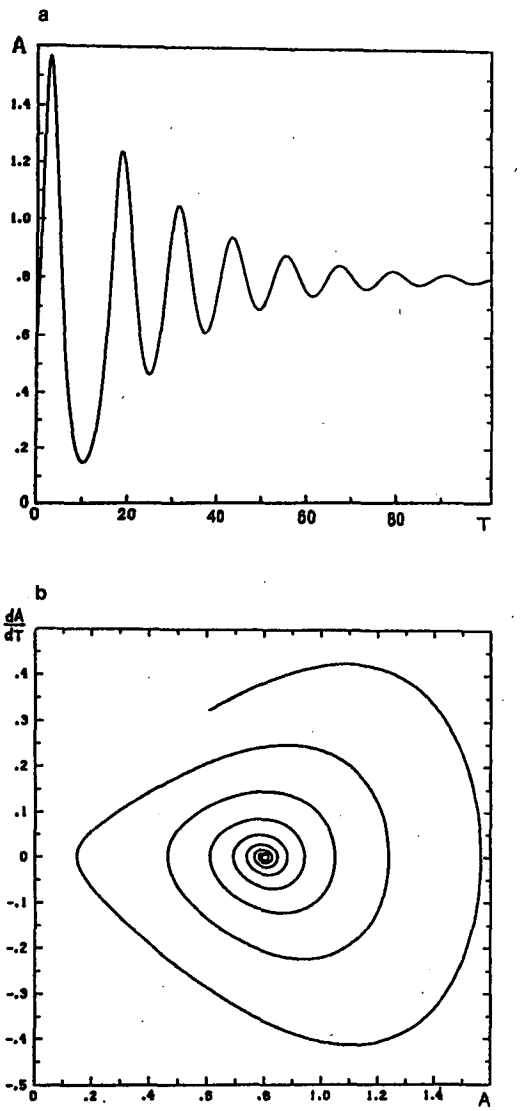

FIG. 3. (a) The time history of the wave amplitude showing the damped oscillatory approach to a steady state. The parameters used in calculation are $k = 1.1$ (wave two), $l = \pi/2$, $\Delta = 0.1$, and $\mu = 0.03$. (b) The phase plane orbit of the solution of Fig. 3a.

5. Application to atmospheric vacillation

Several observational (Miller, 1974; McGuirk and Reiter, 1976; McGuirk, 1982), and numerical studies (Hunt, 1978; Yoden, 1981) suggest that the tropospheric and lower stratospheric vacillation during cold seasons appears to be linked to baroclinic processes, involving primarily planetary, ultralong wave–mean flow interactions. McGuirk's (1982) recent study summarized some interesting features of the vacillation, which are:

1) The zonal available potential energy, $\bar{P}$, has a strong and persistent vacillation; the eddy available potential energy, P', and the kinetic energy, K', vacillate in phase, while being precisely out of phase with $\bar{P}$.

2) The horizontal heat flux, which is poleward most of the time during the vacillation cycle, appears to be in phase with the eddy energy.

3) The smallest vertical wave-tilt occurs at the maximum wave amplitude, while the largest vertical wave-tilt is found at the minimum wave amlitude; the waves *seldom* tilt eastward.

4) Wave two is the dominant vacillating wave component which makes the largest contribution to the eddy energy and to the poleward heat flux.

5) The vacillation period of P and the heat flux is centered around 24 days with a variance of five days; the vacillation period for wave 2 and 3 is about 22–26 days and 19–24 days, respectively.

The present model describes the weakly nonlinear interaction between a single baroclinic, unstable Green mode and the mean flow in the presence of dominant

internal, thermal dissipation. The major results developed in section 3 are summarized as follows. To $O(\epsilon^{3/2})$, the perturbation streamfunction is

$$\phi(x, y, z, T) = \epsilon^{1/2}\Phi(z, T)e^{ikx}\cos ly + \text{c.c.} + O(\epsilon^{3/2}), \tag{5.1}$$

where Φ denotes the complex wave amplitude

$$\Phi(z, T) = e^{pz}\left[A(T)z(1 - \tilde{K}z) - \frac{i}{k}\left(\Delta^{1/2}\frac{dA}{dT} + \mu A\right)(1 - 2\tilde{K}z)\right] \tag{5.2}$$

and the zonally averaged streamfunction is

$$\bar{\psi}(y, z, T) = -yz - \epsilon B(T) \times \sum_{J=1}^{\infty} \frac{f_J(z)}{\left(J - \frac{1}{2}\right)\pi}\sin\left(J - \frac{1}{2}\right)\pi y + O(\epsilon^{3/2}), \tag{5.3}$$

where $f_J(z)$ is defined by (A1). In (5.1) and (5.3) the time dependent parts $A(T)$ and $B(T)$ are governed by amplitude equations (3.12) and (3.13).

The zonal available potential energy in the model channel, for a unit length in the x-direction, is given by

$$\bar{P} = \int_0^{\infty} dz \int_{-1}^{1} dy \frac{\rho_s}{2S}\left(\frac{\partial\bar{\psi}}{\partial z}\right)^2,$$

where the nondimensional density is $\rho_s = e^{-z}$. Using (5.3), we find

$$\bar{P} = \int_0^{\infty} \frac{\rho_s}{2S}\left\{\frac{2}{3} + 4\epsilon B(T) \times \sum_{J=1}^{\infty}(-1)^J\left[\left(J - \frac{1}{2}\right)\pi\right]^{-3}\frac{df_J}{dz}\right\}dz + O(\epsilon^2). \tag{5.4}$$

Using (5.1), we can also express the eddy available potential energy and kinetic energy in the same volume as

$$P' = \int_0^{\infty} dz \int_{-1}^{1} \frac{\rho_s}{2S}\overline{\left(\frac{\partial\phi}{\partial z}\right)^2}dy = \epsilon\int_0^{\infty}\frac{\rho_s}{S}\left|\frac{\partial\Phi}{\partial z}\right|^2 dz + O(\epsilon^2), \tag{5.5}$$

$$K' = \int_0^{\infty} dz \int_{-1}^{1} \frac{\rho_s}{2}\overline{\left[\left(\frac{\partial\phi}{\partial x}\right)^2 + \left(\frac{\partial\phi}{\partial y}\right)^2\right]} = \epsilon\int_0^{\infty}\rho_s(k^2 + l^2)|\Phi|^2 dz + O(\epsilon^2), \tag{5.6}$$

where the overbar denotes an x-average.

The energy equations in the present model can be written as

$$\frac{\partial\bar{P}}{\partial t} = -\langle\bar{P}\cdot P'\rangle + \bar{G},$$

$$\frac{\partial P'}{\partial t} = \langle\bar{P}\cdot P'\rangle - \langle P'\cdot K'\rangle - \epsilon_p',$$

$$\frac{\partial K'}{\partial t} = \langle P'\cdot K'\rangle - \epsilon_k', \tag{5.7}$$

with zonal kinetic energy $\bar{K}$ remaining constant. In (5.7), $\bar{G}$ is the generation of the zonal available potential energy; since we assume that the vertical shear of the basic flow is constant, we are implying implicitly an energy source for the zonal flow; at the equilibrium wave state, $\bar{G} = \epsilon_p' + \epsilon_k'$. The conversion from $\bar{P}$ to P', or from the zonal energy to the eddy energy, is given by

$$\langle\bar{P}\cdot P'\rangle = \int_0^{\infty}\rho_s\,\mathrm{HHF}(z, T)dz, \tag{5.8}$$

where $\mathrm{HHF}(z, T)$ represents horizontal heat flux per unit volume at level z and is defined by

$$\mathrm{HHF}(z, T) = \int_{-1}^{1}\frac{1}{S}\overline{\frac{\partial\phi}{\partial z}\frac{\partial\phi}{\partial x}}dy = \epsilon\frac{2k}{S}|\Phi|^2\frac{\partial}{\partial z}\mathrm{ph}\Phi + O(\epsilon^2), \tag{5.9}$$

where $\mathrm{ph}\Phi$ is the phase of the complex amplitude $\Phi(z, T)$. The conversion from P' to K' is

$$\langle P'\cdot K'\rangle = \int_0^{\infty}\rho_s\,\mathrm{VHF}(z, T)dz, \tag{5.10}$$

where $\mathrm{VHF}(z, T)$ denotes vertical heat flux per unit volume at level z, and may be defined as

$$\mathrm{VHF}(z, T) = \int_{-1}^{1} w\overline{\frac{\partial\phi}{\partial z}}dy = \mathrm{HHF} - \left(2\mu + \Delta^{1/2}\frac{\partial}{\partial T}\right)P' + O(\epsilon^2). \tag{5.11}$$

The dissipation due to Newtonian cooling and due to Ekman layer friction are, respectively,

$$\epsilon_p' = \int_0^{\infty} dz\rho_s\int_{-1}^{1}\frac{\mu}{S}\overline{\left(\frac{\partial\phi}{\partial z}\right)^2}dy = \int_0^{\infty} 2\rho_s\mu P'dz + O(\epsilon^2), \tag{5.12}$$

$$\epsilon_k' = 2\epsilon\rho_s\delta k^2|\Phi|^2|_{z=0}. \tag{5.13}$$

Since $\delta = O(\epsilon)$, and ϵ_k' is order of ϵ^2, and can be neglected when dealing with energetics valid to $O(\epsilon)$.

In (5.9) the quantity $\partial/\partial z(\mathrm{ph}\Phi)$, represents the vertical wave tilt; when positive, the trough or ridge of the wave tilts westward with height, and the horizontal heat flux is poleward, implying conversion from zonal

available potential energy to eddy available potential energy. This quantity is also determined by the phase difference between temperature field and flow field. By using (5.2), we can show that

$$\frac{\partial}{\partial z}(\mathrm{ph}\Phi) = \left(\Delta^{1/2}\frac{d\ln|A|}{dT} + \mu\right) \times \left\{\frac{e^{2pz}[(1-\tilde{K}z)^2 + \tilde{K}^2z^2}{k\left[\left(\varphi_0 + \frac{\Delta^{1/2}}{k}\dot{\theta}\varphi_1\right)^2 + \frac{1}{k^2}\left(\Delta^{1/2}\frac{\dot{R}}{R} + \mu\right)^2\varphi_1^2\right]}\right\}, \tag{5.14}$$

where the braced-quantity is always positive, R and θ are the modulus and phase of A. Therefore, in the presence of $O(\epsilon^{1/2})$ internal dissipation the vertical tilt of the trough or ridge of the finite amplitude Green mode vacillates in phase with dA/dT. As long as

$$\mu > -\Delta^{1/2}\frac{1}{|A|}\frac{d|A|}{dT}, \tag{5.15}$$

the wave will tilt westward, and the corresponding horizontal heat flux will be poleward [see (5.9)]. However, in an inviscid case, or in the case in which the Ekman dissipation is dominant, the wave tilts westward when growing and tilts eastward when decaying; correspondingly, the horizontal heat flux reverses its direction every half period of vacillation. This symmetric pattern of the oscillations of wave tilt and heat flux direction are at odds with the observations. Unlike Ekman dissipation, the internal dissipation does dissipate the potential vorticity in a continuous model. Therefore, even in the decaying stage, a portion of wave energy must be consumed to overcome the dissipation. The direction of the heat flux and the wave tilt are now biased, with westward wave tilt and poleward heat flux being dominant throughout the vacillating cycle. The larger the internal dissipation, the longer the time span in which the wave tilts westward and the heat flux is directed poleward.

Table 1 indicates that for typical cold season atmospheric conditions in the troposphere and stratosphere, the most unstable Green mode ($\Delta = 0.3$) is most likely to be close to wavenumber two around the latitude circle. This fact may explain why wave two is the largest contributor to the eddy energy and the heat flux. The vacillation period had been determined by numerical integration. When μ is small, the vacillation period can also be estimated if we use the inviscid theory. In that limit, the amplitude equations (3.12) and (3.13) reduce to those of Pedlosky (1970) and the nondimensional period of vacillation is given by

$$T_p = \frac{2\sqrt{2}\,K(m^2)}{\sqrt{\chi}\left\{R_0^2 + \frac{k^2C_{0I}^2}{\chi\Delta}\left[1 + \left(1 + \frac{2\chi\Delta}{k^2C_{0I}^2}R_0^2\right)^{1/2}\right]\right\}^{1/2}},$$

TABLE 1. The wavenumber and vacillation period for the most unstable Green mode.

	Case		
	1	2	3
Central latitude of the westerlies (°)	45	40	40
Width of the westerlies (km)	5500	5500	5500
Brunt–Väisälä frequency (10^{-2} s^{-1})	1.7	1.7	1.6
Vertical shear (10^{-3} s^{-1})	1.3	1.6	1.5
Wavenumber around latitude circle of the most unstable Green mode	2.07	2.03	2.07
Vacillation period (inviscid) (days)	24.7	26.1	24.3

where χ is defined by (A3), R_0 is the initial amplitude, and $K(m^2)$ is complete elliptic integral of first kind, the modulus, m, is given by

$$m^2 = \frac{2k^2C_{0I}^2(1 + 2\chi\Delta R_0^2/k^2C_{0I}^2)^{1/2}/\chi\Delta}{R_0^2 + k^2C_{0I}^2[1 + (1 + 2\chi\Delta R_0^2/k^2C_{0I}^2)^{1/2}]/\chi\Delta}.$$

The calculated periods are given in Table 1, where the initial disturbance wave amplitude was assumed to be $1(N_0H^2\lambda_*/f_0)$. The estimated period for the most unstable Green mode is about 3–4 weeks, which is in qualitative agreement with the observations.

Figure 4a shows the time history of $\bar{P}$, P' and K' for wave two, when central latitude is at 45°, the width of the westerlies is 5500 km, the Brunt–Väisälä frequency is 0.017 s^{-1}, the vertical shear is 1.3×10^{-3} s^{-1}, and internal dissipation coefficient is $\mu = 0.05$. It is seen that the eddy available potential energy P' vacillates almost in phase with the kinetic energy K', but precisely out of phase with the zonal available potential energy $\bar{P}$. As shown in Fig. 4b, the $\langle\bar{P}, P'\rangle$ conversion, which also denotes the total horizontal heat flux, also vacillates nearly, but not completely, in phase with P'. Furthermore, the poleward heat flux (positive value) dominates the vacillation cycle, as expected from (5.15). The $\langle P', K'\rangle$ conversion was found to be almost in phase with $\langle\bar{P}, P'\rangle$. The mean flow correction is strongest in the lower stratosphere ($z = 3.5H$), and at this level it varies in phase with $\bar{P}$, while in the troposphere the variation of $\bar{u}$ is much weaker and tends to be out of phase with $\bar{P}$ in lower troposphere (Fig. 4c).

Figure 5 shows the vertical distribution of the horizontal heat flux at different times during one period. The vertical distribution of the poleward heat flux has a double-peak feature, one near ground and other in the lower stratosphere. The major extrema of vertical heat flux are located in the lower troposphere and the middle stratosphere.

It is noticed that the variation of $\langle\bar{P}, P'\rangle$, or heat flux, is not completely in phase with P', but leads by a phase angle less than $\pi/4$. A tentative explanation of

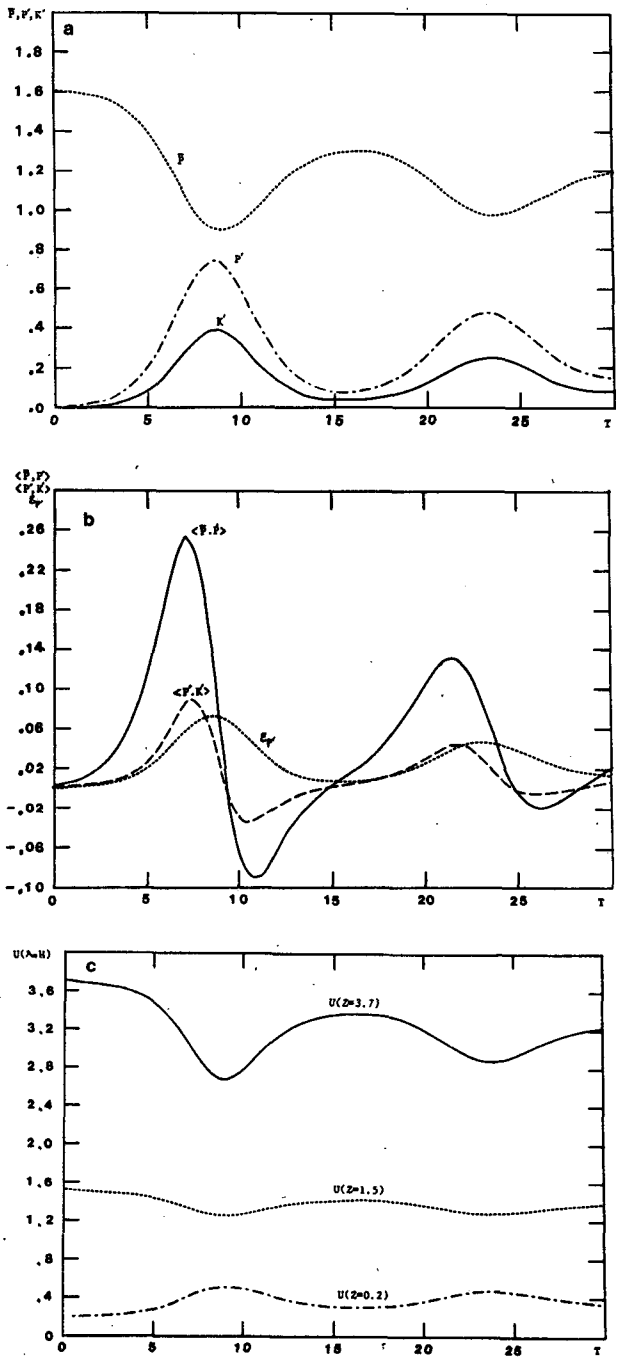

FIG. 4. The time history of (a) the zonal available potential energy $\bar{P}$, the eddy available potential energy P', and the eddy kinetic energy K'; (b) the energy conversion terms $\langle \bar{P}, P' \rangle$ and $\langle P', K' \rangle$, and the dissipation term ϵ_p'; (c) the mean flow correction at z_*/H = 3.7, 1.5 and 0.21, where H is the density scale height.

the phase relation among the energy components $\bar{P}$, P', K', and the conversion terms $\langle \bar{P}, P' \rangle$, $\langle P', K' \rangle$ are given below. Initially $\bar{P}$ is large, the corresponding large latitudinal temperature gradient sets off the development of unstable baroclinic planetary waves. The increase in baroclinic activity strengthens the poleward heat flux and enhances the $\langle \bar{P}, P' \rangle$ conversion. Therefore, eddy available potential energy grows, while zonal available potential energy decreases. The amplifying wave also stimulates the $\langle P', K' \rangle$ conversion, hence K' also grows at this stage. Note that, the nonlinear interaction between the wave and zonal mean flow causes the different phase changes between the temperature field [ph($\partial\Phi/\partial z$)] and the flow field (phΦ), or the variation of the vertical wave-tilt and the $\langle \bar{P}, P' \rangle$ conversion. As a result, the westward wave-tilt, the horizontal heat flux and the related $\langle \bar{P}, P' \rangle$ conversion all reach their maxima in the growing stage. After its maximum, $\langle \bar{P}, P' \rangle$ decreases and the wave growth slows down. As $\langle \bar{P}, P' \rangle$ decreases, by the time when $\langle \bar{P}, P' \rangle = \langle P', K' \rangle + \epsilon_p'$, the growth rate of the wave becomes zero, hence P', K' are maxima, while $\bar{P}$ reaches a minimum. After the P', K' maxima, the heat flux is greatly reduced; $\bar{P}$ begins to grow at this stage, its generation by diabatic heating exceeding its loss by the $\langle \bar{P}, P' \rangle$ conversion provided $\langle \bar{P}, P' \rangle > 0$. Meanwhile, P', K' start to decrease. Once $\bar{P}$ reaches its relatively smaller second maximum, the above process will repeat itself until final equilibrium is achieved.

6. Discussion and concluding remarks

The dynamic regime, which was examined in the context of the weakly nonlinear analysis, considered moderate internal dissipation of $O(\Delta^{1/2})$, that was assumed to dominate over the Ekman dissipation taken as $O(\Delta)$.

When the characteristic dissipative time scale equals the baroclinic development time scale, the evolution of the Green modes eventually leads to steady wave states, that are always stable to small perturbations. No stable limit cycle or aperiodic solutions were found in the realistic parameter ranges that typify atmospheric

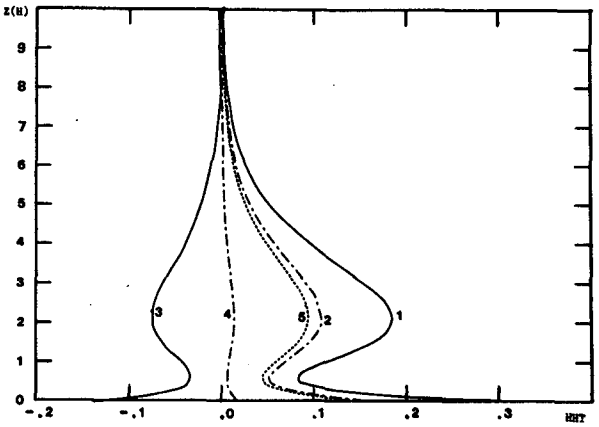

FIG. 5. Vertical distribution of the poleward heat flux at different times in a vacillation cycle: (1) T = 5.6; (2) T = 8.8; (3) T = 12.0; (4) T = 15.6 and (5) T = 19.2.

winter conditions. The evolution of the system as it approaches its steady wave state may exhibit a monotonic or a damped oscillatory behavior, depending upon the relative magnitudes of the inviscid growth rate and of the internal dissipation. Vacillatory behavior occurs, as long as the characteristic dissipative time is longer than $\sqrt{3}/2$ times the e-folding time for baroclinic development. For reasonable atmospheric winter parameters the theory predicts a vacillation period for the most unstable Green mode (wave two) of about several weeks.

The present model shows that as the criterion (4.14) is satisfied, both the amplitude and the phase speed of the finite amplitude Green mode will undergo damped vacillatory behavior. However, the fluctuations of the phase speed are much weaker than the amplitude fluctuations. The theory also predicts that nonlinear interaction between the wave and the mean flow causes different phase variation between the thermal and the flow fields, and the conversion term from zonal available to eddy available potential energy leads the eddy energies by a phase angle less than $\pi/4$; the zonal available potential energy vacillates precisely out of phase with the total eddy energy while the eddy available potential energy is almost in phase with the eddy kinetic energy; for representative winter tropospheric and stratospheric conditions, wave two around the latitude circle is the favorable candidate for the most unstable Green mode, and may make the largest contribution to both the total eddy energy and the horizontal heat flux. Moreover, in the course of its vacillation, the vertical tilt of the constant phase line may remain westward, and the horizontal heat flux may be poleward throughout the entire vacillation cycle, as long as (5.15) is satisfied. These results seem to agree qualitatively with observations, suggesting the importance of the mean flow–baroclinic planetary wave interaction in the vacillation phenomena, that appear to be an inherent property of the general circulation.

The model is rather idealized when compared to the real atmosphere. The description of the Rayleigh dissipation of the potential vorticity in Eq. (2.1) is a crucial assumption. In their nondimensional forms, the Newtonian cooling and horizontal turbulent viscosity can be written as $-\mu(\partial^2/\partial z^2 - \partial/\partial z)\phi$ and $-S\mu_M\nabla^2\phi$, respectively, and therefore the scale dependence does not affect these dissipations in the same manner; also the model excluded the wave–wave interaction mechanism and the meridional variations of the basic flow. There remains the important issue as to how drastically these limitations would change the preceding results and predictions. Although we intended to examine only the free, baroclinic, planetary wave–mean flow interaction, it is realized that the excitation of planetary waves via other mechanisms, as for example, by strong sensible heating due to relatively warm oceans, the presence of forcings due to mountains, etc., should also be considered when one attempts to model atmospheric vacillation. However, we believe that the intrinsic mechanism of the nonlinear interaction remains a fundamental ingredient of the vacillation phenomenon.

Acknowledgments. The authors are grateful to anonymous reviewers for their relevant comments on an earlier version of the manuscript which helped clarify the analysis and presentation of this work. This work, was supported, in part, by National Science Foundation Grant ATM8413545 and NOAA/Princeton University Grant NA84EAD00057; we also gratefully acknowledge support from the FSU Computing Center.

APPENDIX

The Expressions for the Function $f_J(z)$ and the Coefficient χ

The solution for $f_J(z)$ is found to be

$$f_J(z) = -\frac{1}{r_J}(2l^2C_J + 2p\mathcal{S}_0 + \mathcal{S}_1)e^{r_Jz} + (\mathcal{S}_2z^2 + \mathcal{S}_1z + \mathcal{S}_0)e^{2pz} \quad \text{(A1)}$$

where

$$C_J = (-1)^{J+1}2j/(j^2 - 4l^2), \quad j = \left(J - \frac{1}{2}\right)\pi, \quad \text{(A2a)}$$

$$r_J = \frac{1}{2} - \left(\frac{1}{4} + j^2S\right)^{1/2}, \quad \text{(A2b)}$$

$$\mathcal{S}_2 = 8\tilde{K}l^2C_J/(4p^2 - 2p - Sj^2) \quad \text{(A2c)}$$

$$\mathcal{S}_1 = -2\mathcal{S}_2\tilde{K}^{-1} - (8p - 2)\mathcal{S}_2/(4p^2 - 2p - Sj^2) \quad \text{(A2d)}$$

$$\mathcal{S}_0 = \mathcal{S}_2/\tilde{K}^2 - [(4p - 1)\mathcal{S}_1 + 2\mathcal{S}_2]/(4p^2 - 2p - Sj^2) \quad \text{(A2e)}$$

and p is defined by (3.3a).

Coefficient χ in (3.13) is defined by

$$\chi = \frac{\epsilon k^2}{\Delta(\tilde{K} - p)}\left\{-4\tilde{K}l^2I_1 + \sum_{J=1}^{\infty}\frac{(-1)^J4l^2}{j(j^2 - 4l^2)} \times [\mathcal{C}_J(I_{2J} - 1) + (I_{3J} - \mathcal{S}_0)]\right\} \quad \text{(A3)}$$

with

$$I_1 = h^{-6}(h^4 + 8\tilde{K}h^3 + 36\tilde{K}^2h^2 + 96\tilde{K}^3h + 120\tilde{K}^4), \quad \text{(A4a)}$$

$$I_{2J} = -4\tilde{K}(r_J - 2\tilde{K})^{-3} \times [(r_J - 2\tilde{K})^2 + 2\tilde{K}(r_J - 2\tilde{K}) + 2\tilde{K}^2], \quad \text{(A4b)}$$

$$I_{3J} = 4\tilde{K}h^{-5}[-\mathcal{S}_0h^4 + (\mathcal{S}_1 - 2\tilde{K}\mathcal{S}_0)h^3 - 2(\mathcal{S}_2 - 2\tilde{K}\mathcal{S}_1 + \tilde{K}^2\mathcal{S}_0)h^2 + 6(\tilde{K}^2\mathcal{S}_1 - 2\tilde{K}\mathcal{S}_2)h - 24\tilde{K}^2\mathcal{S}_2], \quad \text{(A4c)}$$

$$\mathcal{C}_J = -(2p\mathcal{S}_0 + \mathcal{S}_1 + 2l^2C_J)/r_J, \quad h = 4p - 1$$

and C_J, r_J, $\mathcal{S}_2$, $\mathcal{S}_1$, $\mathcal{S}_0$ are defined by (A2a)–(A2e).

REFERENCES

Arakawa, A., 1961: The variation of the general circulation in the barotropic atmosphere. *J. Meteor. Soc. Japan,* **39,** 49–58.

Brindley, J., and I. M. Moroz, 1980: Lorenz attractor behavior in a continuously stratified baroclinic fluid. *Phys. Lett.,* **77A,** 441–444.

Charney, J. G., 1947: The dynamics of long waves in a baroclinic westerly current. *J. Meteor.,* **2,** 136–163.

Hunt, B. G., 1978: Atmospheric vacillations in a general circulation model I: The large-scale energy cycle. *J. Atmos. Sci.,* **35,** 1133–1143.

Lorenz, E. N., 1963a: The mechanics of vacillation. *J. Atmos. Sci.,* **20,** 448–464.

——, 1963b: The determination of nonperiodic flow. *J. Atmos. Sci.,* **20,** 130–141.

McGuirk, J. P., 1982: The climatology and physical mechanisms of atmospheric vacillation. Tech. Rep., Dept. of Meteor., Texas A&M University.

——, and E. R. Reiter, 1976: A vacillation in atmospheric energy parameters. *J. Atmos. Sci.,* **33,** 2079–2093.

Miller, A. J., 1974: Periodic variation of atmospheric circulation at 14–16 days. *J. Atmos. Sci.,* **31,** 720–726.

Namias, J., 1950: The index cycle and its role in the general circulation. *J. Meteor.,* **7,** 130–139.

Pfeffer, R. L., G. Buzyna and W. W. Fowlis, 1974: Synoptic feature and energetics of wave-amplitude vacillation in a rotating, differentially-heated fluid. *J. Atmos. Sci.,* **31,** 622–645.

Pedlosky, J., 1970: Finite amplitude baroclinic waves. *J. Atmos. Sci.,* **27,** 15–30.

——, 1971: Finite amplitude baroclinic waves with small dissipation. *J. Atmos. Sci.,* **28,** 487–497.

——, 1972: Limit cycles and unstable baroclinic waves. *J. Atmos. Sci.,* **29,** 53–63.

——, 1979: Finite amplitude baroclinic waves in a continuous model of the atmosphere. *J. Atmos. Sci.,* **36,** 1908–1924.

——, 1980: Chaotic and periodic behavior of finite-amplitude baroclinic waves. *J. Atmos. Sci.,* **37,** 1177–1196.

Quinet, A., 1974: A numerical study of vacillation. *Advances in Geophysics,* Vol. 17, Academic Press, 101–186.

Yoden, S., 1981: Quasi-periodic energy variation in a zonal flow-baroclinic wave interaction model. *J. Meteor. Soc. Japan,* **59,** 291–302.

Wang, B., 1982: Evolution of the diabatic finite amplitude ultralong waves and extended-long range variation of the general circulation. *Sci. Sin.,* **25B,** 1312–1325.

——, A. Barcilon and L. N. Howard, 1985: Linear dynamics of the transient planetary waves in the presence of damping. *J. Atmos. Sci.,* **42,** 1893–1910.

Webster, P. J., and Keller, J. L., 1975: Atmospheric variations: Vacillations and index cycles. *J. Atmos. Sci.,* **32,** 1283–1300.